ELSEVIER

Chemical Physics 262 (2000) 53–63

Chemical Physics

www.elsevier.nl/locate/chemphys

Probing the electronic structure of iron clusters using photoelectron spectroscopy

Lai-Sheng Wang [a,b,*], Xi Li [a,b], Hai-Feng Zhang [a,b]

[a] *Department of Physics, Washington State University, 2710 University Drive, Richland, WA 99352, USA*

[b] *W.R. Wiley Environmental Molecular Sciences Laboratory, MS K8-88, Pacific Northwest National Laboratory, Richland, WA 99352, USA*

Received 9 October 2000

Abstract

The electronic structure of small iron clusters, Fe_n^- ($n = 3$–34), was investigated using size-selected anion photoelectron spectroscopy at three photon energies: 355, 266, and 193 nm. Temperature-dependent studies were performed for selected clusters at 355 nm. The spectra of cold clusters at 355 nm revealed well-resolved electronic transitions. An unusually sharp threshold peak was observed for a number of clusters, particularly for $n = 12$–15. The electronic structure variations as a function of size were found to correlate well with changes in the cluster chemical reactivity in the same size ranges. The 193-nm photoelectron spectra, which provided a broader range of valence band electronic structures for the clusters, were compared to bulk photoemission spectra. The electronic structure revealed at 193 nm was found to exhibit bulk-like behavior starting at Fe_{25}. This observation was also consistent with the size dependence of the cluster electron affinities, ionization potentials, and chemical reactivity, which all showed more smooth size variations above Fe_{25}. It was also shown that the obtained electronic structure information from the well-resolved photoelectron spectra will be valuable to compare with and verify ab initio calculations in order to completely understand the chemical, structural, and magnetic properties of the iron clusters. © 2000 Published by Elsevier Science B.V.

1. Introduction

Clusters containing a few to few thousand atoms occupy an intermediate size regime between individual atoms and bulk condensed matters [1,2]. In this size regime, the properties of the clusters are strongly size dependent, giving rise to the quantum size effects. The electronic structure of clusters and its size evolution are among the most important questions in cluster science. The electronic structure of a cluster determines its chemical and physical properties, such as reactivity, magnetic and optical properties. For small clusters, we expect that their electronic structure will be molecular-like with discrete energy levels. As the cluster size increases, the density of electronic energy levels will increase and become bulk-like band structures at some critical size range. Key issues in studying the electronic structure of clusters involve the elucidation of how the electronic structure evolves with cluster size, when it approaches the bulk limit, and how it is related to their other chemical and physical properties.

* Corresponding author. Address: Department of Physics, Washington State University, 2710 University Drive, Richland, WA 99352, USA. Tel.: +1-509-376-8709; fax: +1-509-376-6066.
E-mail address: ls.wang@pnl.gov (L.-S. Wang).

0301-0104/00/$ - see front matter
PII: S0301-0104(00)00351-7

One of the most powerful experimental techniques to probe the electronic structure of clusters is photoelectron spectroscopy (PES) of size-selected anions. In this technique, kinetic energies of photoemitted electrons from a size-selected cluster anion are measured, yielding direct information about the electronic energy levels (DOS: density of states) of the corresponding neutral cluster. Different versions of PES techniques have been used in a number of research groups to investigate the electronic structure of clusters [3–14]. Using a state-of-the-art magnetic-bottle time-of-fight (TOF)-PES apparatus with a laser vaporization cluster source [10,15], we have studied clusters of a variety of materials, including transition metals [10,15–21], metal and semiconductor oxides [22–32], metal carbides [33–38], and simple free-electron metals [39–42], with a range of photon energies. At low photon energies and for small clusters, vibrational information has also been obtained. Using high photon energies, we can probe more deeply into the valence band of clusters and can obtain electronic structure information that can be directly compared to valence-band photoemission spectra of bulk materials.

Of particular relevance to the current paper are our previous works on transition metal clusters [10,15–21], for which we have focused on the early 3d elements, Ti, V, and Cr. We obtained photoelectron spectra for clusters containing up to 70 atoms and at various photon energies. These results were reviewed previously [15]. Essentially we found that the electronic structures of these clusters approach the bulk rather rapidly. For Ti clusters [17], we observed no fine features above Ti_{10}. For V clusters [18], we observed that bulk-like features appear at V_{17} and the cluster spectra become almost identical to that of the bulk beyond about V_{50}. For Cr clusters [19,20], we found a dimer-like growth path from Cr_2 to Cr_{10} and that bulk-like PES features appear at about Cr_{25}. We have also studied clusters of the late 3d elements [10,15,16,21], but only at low photon energies and in the small size regime. Small cobalt and nickel clusters have also been the subjects of several other PES investigations [43–46].

Clusters of iron represent one of the most extensively studied transition metal cluster systems experimentally. Their chemical reactivity was shown to exhibit a strong size effect [47–56]. In particular, their reactivity with H_2 shows a striking size dependence with orders of magnitude variations in reaction rate between Fe_{15} and Fe_{16}, Fe_{18} and Fe_{19}, and, to a less extent, between Fe_{22} and Fe_{23} [49]. Because of the unique ferromagnetic properties of bulk iron, studies on the magnetic properties of iron clusters have also drawn considerable interests [57–60]. All iron clusters were found to be magnetic with higher moments than the bulk. In other experiments, ionization potentials (IPs) and dissociation energies of the positive clusters were measured [61–64]. There have also been several recent studies on chemisorbed neutral Fe clusters [65,66] and on the chemical reactivity of Fe_n^+ clusters [67,68].

Theoretically, a number of studies have attempted to understand the electronic and atomic structures of small iron clusters [69–80]. However, the complicated nature of these systems only allows a few selected high symmetry and very small systems to be studied in the early efforts [69–75]. Recently, there have been several ab initio studies on small iron clusters, consisting of a few atoms [76–80].

Our previous PES studies on the Fe clusters covered a small size range (up to Fe_{24}) and only at 3.496 eV photon energy (355 nm) [10,16]. The emphasis of the previous investigations was to correlate the electronic structure information obtained from the PES data to the chemical reactivity of the clusters, with the aid of extended Huckel calculations. In the present paper, we report a more extensive study of Fe clusters for up to 34 atoms and at three photon energies (355, 266, and 193 nm). In particular, we conducted temperature-dependent studies and obtained significantly improved data at 355 nm for relatively cold clusters. The goal of the current study is to elucidate the evolution of the Fe cluster electronic structure to the bulk limit and to compare and correlate further the electronic structure information obtained here to other properties of the Fe clusters, such as IPs and chemical reactivity, as well as available theoretical results from more recent studies. The data at the higher photon energies allow us to compare directly to bulk photoemission results.

2. Experimental

Details of the experimental apparatus used for this study have been published previously [10,15] and a schematic drawing is shown in Fig. 1. It consists of a laser vaporization cluster source, a TOF mass spectrometer, and a magnetic-bottle TOF-PES analyzer. The iron cluster anions were produced using laser vaporization of a pure iron target. The second harmonic output (532 nm) from a Q-switched Nd:YAG laser was used as the vaporization laser. The vaporization laser beam (10 mJ/pulse) was focused down to a 1-mm-diameter spot onto a pure iron disk target, which is controlled by two stepping motors. Two pulsed-valves (R.M. Jordan Com., CA) were used simultaneously to deliver an intense pulse of helium carrier gas (10 atm backing pressure), which was synchronized with the vaporization laser pulse. The clusters entrained in the carrier gas underwent a supersonic expansion and were skimmed by a 6-mm-diameter skimmer to form a collimated beam. The anions in the beam were extracted perpendicularly by a high voltage pulse into the TOF mass spectrometer for size analyses. The desired clusters were size selected by a mass gate and decelerated by a momentum decelerator before being detached by a detachment laser beam in the interaction zone of the magnetic-bottle PES apparatus. In the current experiment, a Nd:YAG laser (355 and 266 nm) and an excimer laser (193 nm) were used for the photodetachment. Photoelectrons emitted in nearly all 4π solid angles were collected and analyzed by a 3.5-m-long electron flight tube. The experiments were performed at 10 Hz repetition rates at 355 nm and 20 Hz repetition rates at 266 and 193 nm with the cluster beam off at alternating laser shots for background subtraction. Photoelectron kinetic energy spectra were obtained from the measured TOF spectra, calibrated by the known spectrum of Cu^-. The reported binding energy spectra were obtained by subtracting the kinetic energy spectra from the photon energies. The resolution of the spectrometer was better than 30 meV for 1 eV electron kinetic energy. Higher resolution spectra were obtained at lower photon energies, whereas more deeply bound electrons were probed at higher photon energies at the expense of energy resolution.

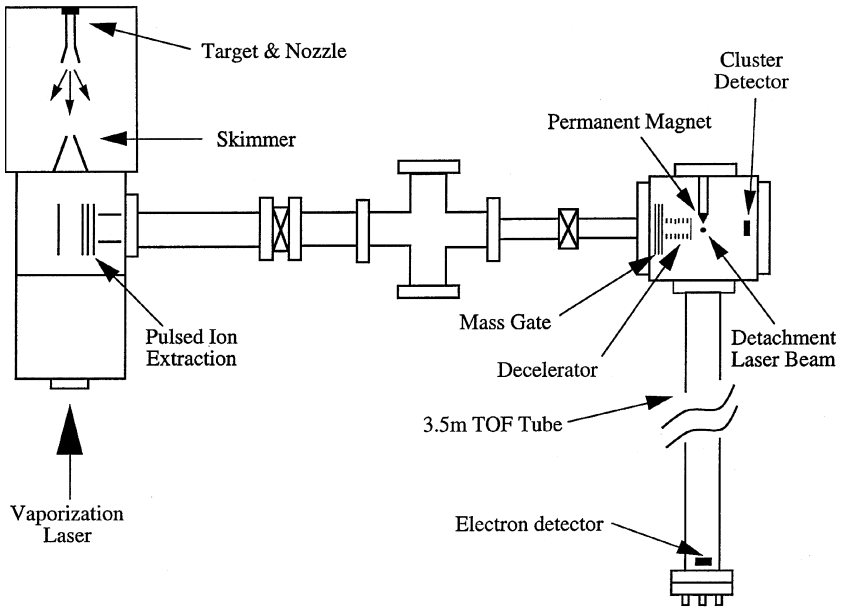

Fig. 1. Schematic drawing of the laser vaporization/magnetic-bottle TOF-PES apparatus.

3. Results

3.1. Photoelectron spectra at 355 nm (3.496 eV)

The 355-nm PES spectra of Fe_n^- ($n = 3$–29) are shown in Fig. 2. The spectra were significantly better resolved than those that we reported previously in the size range from Fe_3^- to Fe_{24}^- [10,16]. We found that two factors were critical to obtain the improved data: (1) cluster temperature and (2) detachment laser fluence. As we reported recently [42,81], we can control the cluster temperatures to some degree by carefully choosing the clusters with longer resident times in the cluster nozzle. Fig. 3 shows a set of data for Fe_n^- ($n = 12$–15) at two different temperature regimes. For the iron clusters, we found that high laser fluences also caused broadening of the PES spectra due to multiphoton effects [82,83]. For all the data presented in Figs. 2 and 3, we used a very low laser fluence of ~0.3 mJ/cm^2 (pulse width ~ 7 ns). Under the current experimental conditions, more fine features were resolved for the larger clusters. Most notably, the sharp and strong threshold feature in the spectra of Fe_{10}^- to Fe_{15}^- was especially well resolved.

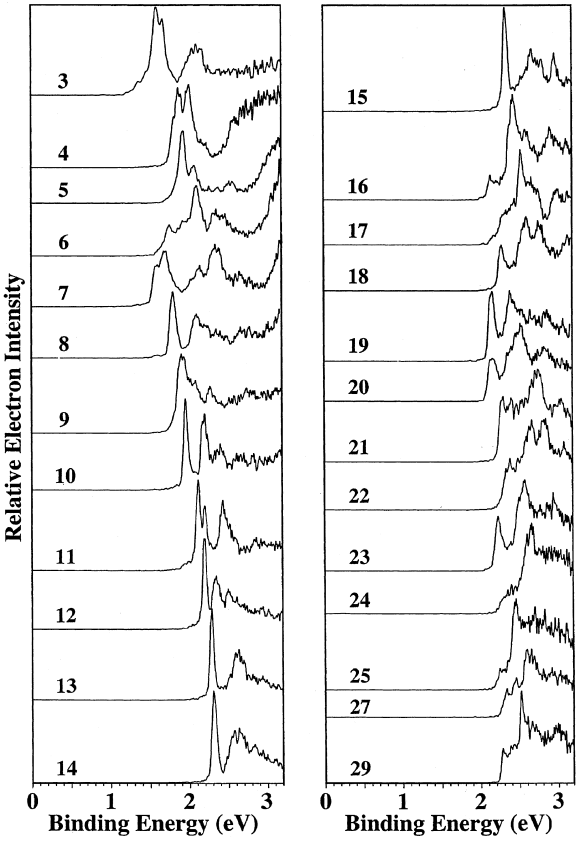

Fig. 2. Photoelectron spectra of Fe_n^- ($n = 3$–29) at 355 nm (3.496 eV).

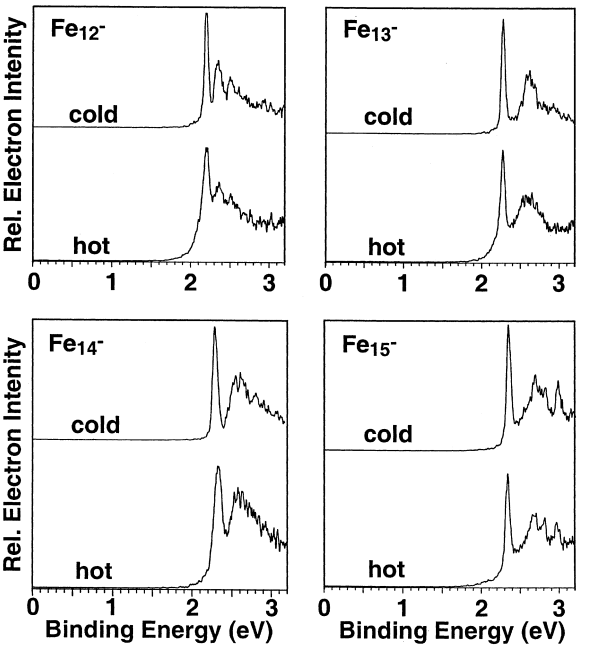

Fig. 3. Photoelectron spectra Fe_n^- ($n = 12$–15) at 355 nm, measured at two temperature regimes, demonstrating the broadening effects for hot clusters.

The adiabatic electron affinities (EAs) for the neutral clusters were estimated from the 355-nm spectra and are given in Table 1. The EAs were evaluated by drawing a straight line at the leading edge of the PES spectra and then adding a constant of 0.05 eV to the intersect with the binding energy axis to take account of the resolution and a thermal effect. Within the experimental uncertainty, the values given in Table 1 are consistent with our previous results in the size range of Fe_3–Fe_{24} [10]. The better spectral resolution in the current experiment resulted in slightly more accurate EAs.

Table 1
Adiabatic EA in eV of Fe_n ($n = 3$–34) clusters (uncertainty: ±0.06 eV)

n	EA
3	1.43
4	1.78
5	1.84
6	1.58
7	1.50
8	1.76
9	1.80
10	1.90
11	2.03
12	2.14
13	2.24
14	2.26
15	2.28
16	2.09
17	2.16
18	2.22
19	2.11
20	2.10
21	2.22
22	2.23
23	2.15
24	2.22
25	2.18
26	2.22
27	2.24
28	2.25
29	2.23
30	2.30
31	2.34
32	2.37
33	2.43
34	2.49

3.2. Photoelectron spectra at 266 nm (4.661 eV)

The PES spectra of Fe_n^- ($n = 3$–30) at 266 nm are shown in Fig. 4. The 266-nm photon extended the binding energy range by more than 1 eV relative to that at 355 nm. However, the spectral resolution was clearly reduced at 266 nm due to the electron-energy-dependent spectral resolution of TOF-type electron analyzers, which favor low energy electrons. In addition, the 266-nm photon was just high enough to induce background noises due to surface emission by scattered photons. The poor signal-to-noise ratio in the small cluster size range in the 266-nm spectra was due to these noises. The rising tail in the high binding energy

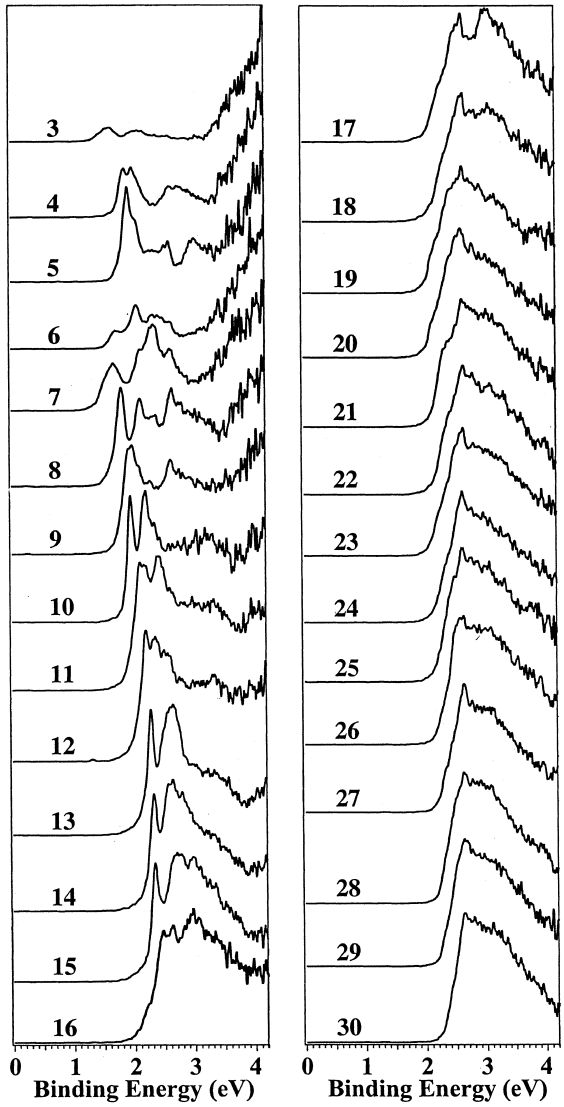

Fig. 4. Photoelectron spectra of Fe_n^- ($n = 3$–30) at 266 nm (4.661 eV).

side in the small clusters was due to a multiphoton process, that induced "thermionic-like" emissions from the cluster anions. Such processes have been observed in previous PES studies of C_{60}^- [82] and other metal clusters [83] and they were especially severe for small clusters and at high photon fluxes.

The sharp threshold features that were resolved in the smaller clusters from Fe_{10}^- to Fe_{15}^- at 355 nm were clearly broadened, due to the increased electron kinetic energies corresponding to these

features at 266 nm. In addition, their relative intensity seemed to be decreased in the 266-nm spectra compared to that in the 355-nm spectra. For clusters above Fe_{15}^-, no distinct features could be resolved in the 266-nm spectra.

3.3. Photoelectron spectra at 193 nm (6.424 eV)

To probe further into the valance band of the Fe clusters, we obtained PES spectra at 193 nm, which are shown in Fig. 5 for Fe_n^- ($n = 4$–34). The noise problem became even more severe at 193 nm, as shown clearly by the poor signal-to-noise ratio in the high binding energy side, particularly, for the small clusters. Understandably, the resolution was further deteriorated at 193 nm. The sharp threshold feature in the 355-nm spectra of Fe_{10}^- to

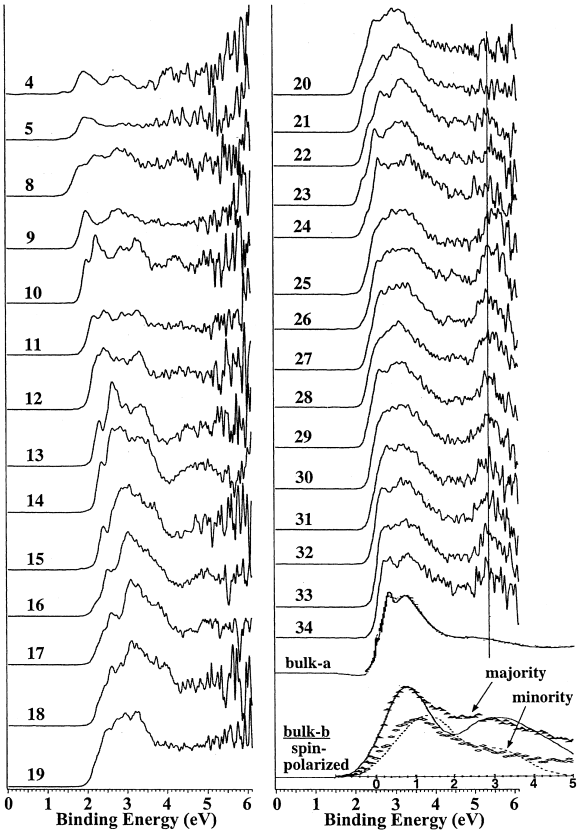

Fig. 5. Photoelectron spectra of Fe_n^- ($n = 4$–34) at 193 nm (6.424 eV), compared to two bulk spectra: bulk-a [85] and bulk-b [86] (see text).

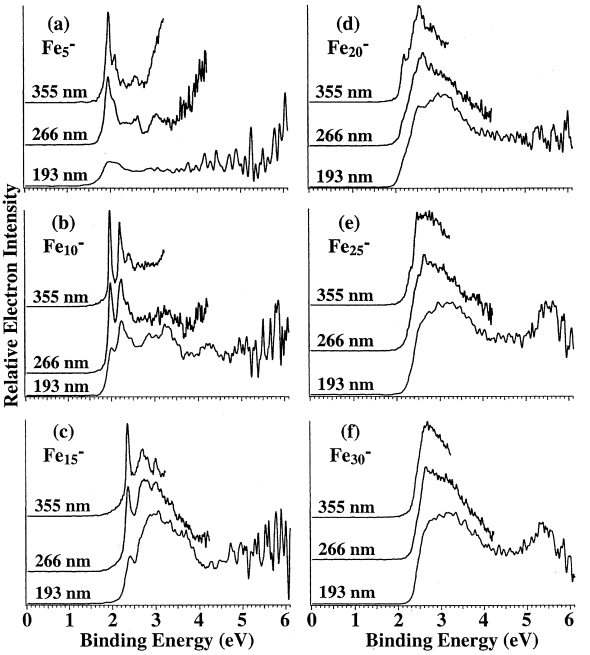

Fig. 6. Comparison of the photon-energy-dependent photoelectron spectra of (a) Fe_5^-, (b) Fe_{10}^-, (c) Fe_{15}^-, (d) Fe_{20}^-, (e) Fe_{25}^-, and (f) Fe_{30}^-.

Fe_{15}^- became shoulders in the 193-nm spectra and their intensity was further reduced. The 193-nm spectra did not reveal much new information for the small clusters, where rather noisy and almost continuous signals seemed to be the dominating characteristics in the high binding energy range. For larger clusters above Fe_{19}^-, the overall spectral pattern seemed to show very little variation with size, consistent with the data at 266-nm. The broad band shape in the 193-nm spectra appeared to show some variations relative to those in the 266-nm spectra, probably due to the photon energy dependence of different electronic transitions contained in the broad band or more likely due to a slight discrimination for low energy electrons in our electron analyzer. To show more clearly this effect, we compared the PES spectra of several clusters at the three photon energies in Fig. 6.

The most interesting features in the 193-nm spectra were the appearance of a new band at about 5.5 eV binding energy starting at Fe_{25}^-. Even though there were continuous signals in the high

binding energy ranges in the spectra of the smaller clusters, the new band seemed to appear rather abruptly at Fe_{25}^-. As shown in Fig. 5 and will be discussed below, the new band in the clusters coincide with a similar bulk photoemission feature. In fact, the whole cluster PES spectra starting from Fe_{25}^- begin to show some similarity to the bulk photoemission spectra.

4. Discussion

4.1. Electron affinity vs. size and comparisons to ionisation potentials and chemical reactivity

The PES spectra of Fe_n^- exhibit dramatic size dependence in the small size regime. These spectra, representing photodetachment transitions from the anion ground state to the ground and excited states of the neutral clusters, provide direct electronic structure information about the neutral clusters. Detailed understanding of these data should provide a basis for elucidating the physical, chemical, and structural properties of the iron clusters. In our previous studies [10,16], we attempted to use extended Huckel calculations to provide a qualitative understanding of the data and help rationalize the observed dramatic size dependence of the chemical reactivity of the small iron clusters. There is indeed an excellent correlation between the PES spectral changes and the chemical reactivity changes as a function of size. For example, dramatic changes of chemical reactivity with H_2 had been observed previously between Fe_{15} and Fe_{16}, Fe_{18} and Fe_{19}, and Fe_{22} and Fe_{23} [49,50]. In the same size ranges we observed significant changes in the PES spectra of the corresponding clusters, as shown most clearly in the 355-nm spectra (Fig. 2).

Fig. 7 shows the measured EAs for the Fe_n clusters as a function of size, compared to their IPs in the same size range from Ref. [61]. Clearly, both the EAs and IPs exhibit large size variations in the smaller size regime from the atom to about Fe_{25}, beyond which the variations with size are relatively small and smooth. Interestingly, the largest chemical reactivity changes also happen in the same size range up to Fe_{25}, becoming more smooth at larger sizes [49]. Although the magnetic moments of the Fe clusters were measured for up to 700 atoms [57–60], no detailed atom-by-atom measurements in the small size regime are yet available. It would be interesting to see whether similar dramatic size variations in the same size

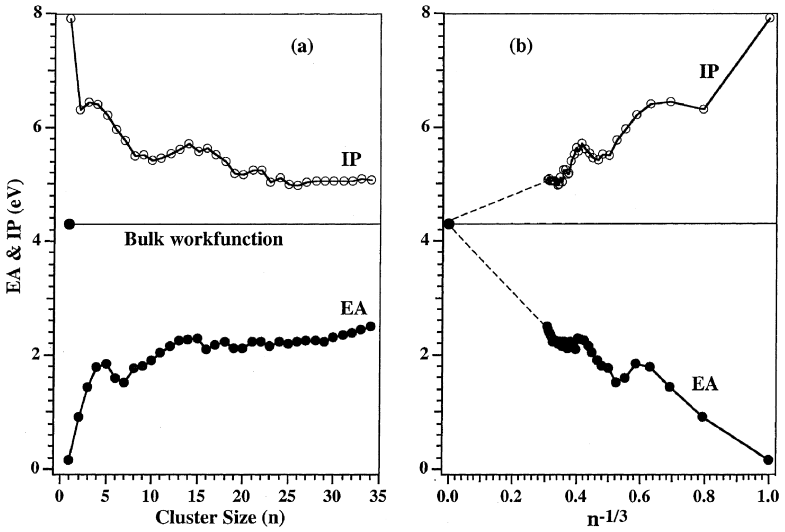

Fig. 7. (a) EA of Fe_n ($n = 1$–34) clusters as a function of size, compared to the corresponding IP; (b) EA and IP of Fe_n ($n = 1$–34) as a function of $n^{-1/3}$. The IP values are from Ref. [61]. The EA of Fe is from Ref. [87] and that of Fe_2 is from Ref. [3]. The bulk workfunction is indicated by the horizontal line.

range would occur in the cluster magnetic moments and whether their size evolution would become smooth and gradual above Fe_{25}.

Fig. 7 also shows that the EAs in general increase with size and approach the bulk workfunction from below, whereas the IPs decrease with size and approach the workfunction from above. The classical metallic droplet model is usually used to describe the changes of IPs or EAs as a function of size [84]. The metallic droplet model predicts a linear dependence of the IPs or EAs on $1/R$, where R is the radius of the cluster. Since R is proportional to the cubic root of the cluster size, we plotted the IPs and EAs vs. $n^{-1/3}$ in Fig. 7b. It seems that the EAs begin to follow the metallic droplet model around Fe_{20}, although that is not the case for the IPs. When or whether the EAs obey the metallic droplet model is strongly dependent on the nature of the bonding and the structures of the clusters. Previously, we found that for V_n clusters the EAs follow the metallic droplet model starting at V_{17}, coinciding exactly with the appearance of bulk-like electronic features in the PES spectra [18].

4.2. Evolution of electronic structure vs. size and appearance of bulk-like features

The 193-nm spectra of Fe_n^- showed very little resolved fine features in the large size range, due to both the increased density of electronic states in the clusters and the limited energy resolution. The only significant PES spectral pattern changes in the large clusters was the appearance of a new PES band near 5.5 eV at Fe_{25}^- (Fig. 5). This band seemed to remain the same in the larger clusters. In fact, the whole spectral pattern did not seem to change much in the larger clusters beyond Fe_{25}^- under the resolution at 193 nm.

Interestingly the PES spectra of the large clusters beyond Fe_{25}^- seemed to exhibit some similarity to photoemission spectra from bulk Fe, in spite of the fact that the EAs of the clusters are still more than 1 eV smaller than the bulk workfunction (Fig. 7). In Fig. 5, two bulk photoemission spectra are compared to the cluster spectra. The bulk spectra were plotted in reference to the Fermi level, but have the same energy scales as the cluster spectra. The first spectrum (bulk-a) is a high resolution, spin-integrated, normal photoemission spectrum from an Fe(1 1 0) surface at room temperature and 21.22 eV photon energy [85]. This high resolution spectrum showed fine features in the broad band near the Fermi level and a second broad band about 3 eV below the Fermi level. The second bulk spectrum (bulk-b) is a low resolution, spin-polarized spectrum from a polycrystalline iron film [86]. This spectrum shows that the band 3 eV below the Fermi level consists mostly of the majority spins. The similarity between the cluster spectra and the bulk spectra are obvious. The 5.5 eV PES feature of the large clusters occurs at the same relative energy position as the second band of the bulk spectra, as shown in Fig. 5 by the vertical line.

These results suggest that the electronic structure of the iron clusters seems to approach the bulk starting at Fe_{25}. This conclusion is consistent with the observations that the EAs, IPs, and chemical reactivity of the iron clusters all showed very smooth and gradual size variations beyond $\sim Fe_{25}$. Our previous investigations of the 3d metal clusters indicated that the onset of bulk-like electronic structures occurs at $\sim Ti_{10}$ for Ti clusters [17], V_{17} for V clusters [18], and Cr_{25} for Cr clusters [20]. Thus, it seems that the 3d transition metal clusters become bulk-like or metallic at rather small size ranges probably due to their high density of electronic states.

4.3. Comparison of photoelectron spectrum of Fe_7^- with theoretical density of states

The well-resolved PES spectra in the small Fe clusters contain detailed electronic structure information of the clusters. Although there have been extensive theoretical works on small iron clusters [69–80], there have been few ab initio studies on their electronic and atomic structures due to their enormous complexity. In our previous studies of the Fe clusters, the extended Huckel model was used to give a very qualitative understanding of the observed PES features with fixed cluster structures [10,16]. However, a complete understanding of the electronic and atomic structures of the small Fe clusters will require high level ab initio calculations and comparisons between

the high level results with the experiments. The PES data can be viewed to represent the DOS of the neutral clusters if the geometrical relaxations are not too great between the anions and the neutral clusters. However, few ab initio data of this kind are available except for several very small Fe clusters.

Castro studied the structural, electronic, and magnetic properties of Fe clusters up to Fe_7 [80]. The Fe_7 cluster was found to be a distorted pentagonal bipyramid with a very high magnetic moment. Specifically, the spin-polarized and total DOS of this cluster was calculated. In Fig. 8, the theoretical results were compared to our measured PES spectrum of Fe_7^-. The structure of Fe_7 and its local magnetic moments are also shown in Fig. 7. The similarity between the experimental PES data and the calculated total DOS is quite clear, providing considerable credence for the underlying cluster structure. It would be very desirable to carry out ab initio calculations of this type for different isomers of a given cluster size and compare with the experimental electronic structure information contained in the high resolution PES data in order to completely elucidate the electronic, structural, chemical, and magnetic properties of these cluster systems.

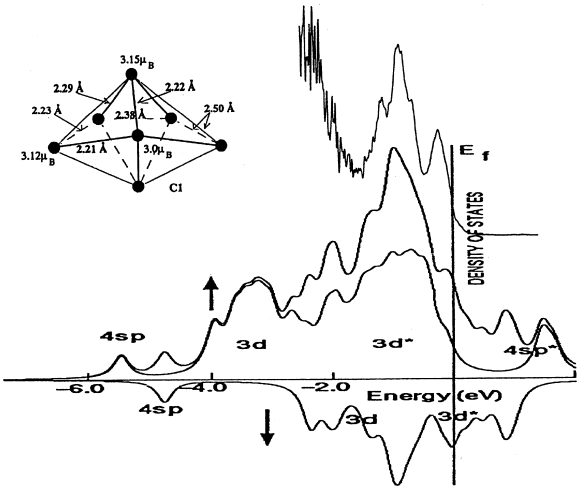

Fig. 8. Comparison of the photoelectron spectrum of Fe_7^- to the calculated DOS of Fe_7 [80]. From top to bottom: PES spectrum of Fe_7^-, total DOS, α-spin DOS, and β-spin DOS. The structure and local magnetic moments of Fe_7 are also shown.

5. Conclusions

We present a comprehensive PES study of size-selected Fe_n^- ($n = 3$–34) clusters at variable photon energies: 355, 266, and 193 nm. The PES spectra yielded detailed electronic structure information for the small iron clusters and their evolution as a function of size. The lower photon energy spectra at 355 nm gave much better resolved spectra while the 193-nm spectra allowed high binding energy features to be accessed. The latter was quite important in order to probe a wide enough valence band range of the clusters to facilitate comparison with bulk photoemission data. We found that the changes of the cluster electronic structure with size correlate well with their size-dependent chemical reactivity. More interestingly, we found that the electronic structure of the iron clusters seem to show bulk-like features starting at about Fe_{25}, consistent with the observations that the EAs, IPs, and chemical reactivity of the iron clusters all show dramatic size variations up to about Fe_{25}, beyond which the size variations in these properties all become more smooth and gradual. The well-resolved PES data provide detailed electronic structure information, which will be valuable to compare to accurate ab initio calculations.

Acknowledgements

This work was supported by the National Science Foundation (CHE-9817811) and performed at the W.R. Wiley Environmental Molecular Sciences Laboratory, a national scientific user facility sponsored by Department of Energy's Office of Biological and Environmental Research and located at Pacific Northwest National Laboratory. Pacific Northwest National Laboratory is operated for the U.S. Department of Energy by Battelle. L.S.W. is an Alfred P. Sloan Foundation Research Fellow.

References

[1] M.A. Duncan (Ed.), Advances in Metal and Semiconductor Clusters, vols. I–IV, JAI Press, Greenwich, 1993–1998.

[2] G. Scoles (Ed.), The Chemical Physics of Atomic and Molecular Clusters, North-Holland, Amsterdam, 1990.
[3] D.G. Leopold, W.C. Lineberger, J. Chem. Phys. 81 (1986) 51.
[4] O. Cheshnovsky, S.H. Yang, C.L. Pettiette, M.J. Craycraft, R.E. Smalley, Rev. Sci. Instrum. 58 (1987) 2131.
[5] K.M. McHugh, J.G. Eaton, G.H. Lee, H.W. Sarkas, L.H. Kidder, J.T. Snodgrass, M.R. Manaa, K.H. Bowen, J. Chem. Phys. 91 (1989) 3792.
[6] M.J. DeLuca, B. Niu, M.A. Johnson, J. Chem. Phys. 88 (1988) 5857.
[7] G. Gantefor, K.H. Meiwes-Broer, H.O. Lutz, Phys. Rev. A 37 (1988) 2716.
[8] T.N. Kitsopoulos, C.J. Chick, Y. Zhao, D.M. Neumark, J. Chem. Phys. 95 (1991) 1441.
[9] H. Handschuh, G. Gantefor, W. Eberhardt, Rev. Sci. Instrum. 66 (1995) 3838.
[10] L.S. Wang, H.S. Cheng, J. Fan, J. Chem. Phys. 102 (1995) 9480.
[11] S.M. Casey, D.G. Leopold, J. Phys. Chem. 97 (1993) 816.
[12] Y. Negishi, H. Kawamata, F. Hayakawa, A. Nakajima, K. Kaya, Chem. Phys. Lett. 294 (1998) 370.
[13] M. Iseda, T. Nishio, S.Y. Han, H. Yoshida, A. Terasaki, T. Kondow, J. Chem. Phys. 106 (1997) 2182.
[14] R. Busani, M. Folkers, O. Cheshnovsky, Phys. Rev. Lett. 81 (1998) 3836.
[15] L.S. Wang, H. Wu, in: M.A. Duncan (Ed.), Advances in Metal and Semiconductor Clusters, vol. IV, Cluster Materials, JAI Press, Greenwich, 1998, p. 299.
[16] L.S. Wang, H.S. Cheng, J. Fan, Chem. Phys. Lett. 236 (1995) 57.
[17] H. Wu, S.R. Desai, L.S. Wang, Phys. Rev. Lett. 76 (1996) 212.
[18] H. Wu, S.R. Desai, L.S. Wang, Phys. Rev. Lett. 77 (1996) 2436.
[19] H.S. Cheng, L.S. Wang, Phys. Rev. Lett. 77 (1996) 51.
[20] L.S. Wang, H. Wu, H. Cheng, Phys. Rev. B 55 (1997) 12884.
[21] L.S Wang, H. Wu, Z. Phys. Chem. 203 (1998) 45.
[22] L.S. Wang, in: C.Y. Ng (Ed.), Advanced Series in Physical Chemistry. Photoionization and Photodetachment, vol. 10, World Scientific, Singapore, 2000 (Chapter XVI).
[23] J. Fan, J.B. Nicholas, J.M. Price, S.D. Colson, L.S. Wang, J. Am. Chem. Soc. 117 (1995) 5417.
[24] J.B. Nicholas, J. Fan, H. Wu, S.D. Colson, L.S. Wang, J. Chem. Phys. 102 (1995) 8277.
[25] L.S. Wang, H. Wu, S.R. Desai, L. Lou, Phys. Rev. B 53 (1996) 8028.
[26] H. Wu, S.R. Desai, L.S. Wang, J. Am. Chem. Soc. 118 (1996) 5296.
[27] L.S. Wang, H. Wu, S.R. Desai, Phys. Rev. Lett. 76 (1996) 4853.
[28] S.R. Desai, H. Wu, C. Rohfling, L.S. Wang, J. Chem. Phys. 106 (1997) 1309.
[29] H. Wu, S.R. Desai, L.S. Wang, J. Phys. Chem. A 101 (1997) 2103.
[30] L.S. Wang, J.B. Nicholas, M. Dupuis, H. Wu, S.D. Colson, Phys. Rev. Lett. 78 (1997) 4450.
[31] H. Wu, L.S. Wang, J. Chem. Phys. 107 (1997) 8221.
[32] H. Wu, X. Li, X.B. Wang, C.F. Ding, L.S. Wang, J. Chem. Phys. 109 (1998) 449.
[33] L.S. Wang, S. Li, H. Wu, J. Phys. Chem. 100 (1996) 19211.
[34] L.S. Wang, H. Cheng, Phys. Rev. Lett. 78 (1997) 2983.
[35] S. Li, H. Wu, L.S. Wang, J. Am. Chem. Soc. 119 (1997) 7417.
[36] X.B. Wang, C.F. Ding, L.S. Wang, J. Phys. Chem. A 101 (1997) 7699.
[37] L.S. Wang, X.B. Wang, H. Wu, H.C. Cheng, J. Am. Chem. Soc. 120 (1998) 6556.
[38] X. Li, L.S. Wang, J. Chem. Phys. 111 (1999) 8389.
[39] X. Li, H. Wu, X.B. Wang, L.S. Wang, Phys. Rev. Lett. 81 (1998) 1909.
[40] S.K. Nayak, B.K. Rao, P. Jena, X. Li, L.S. Wang, Chem. Phys. Lett. 301 (1999) 379.
[41] A.I. Boldyrev, J. Simons, X. Li, L.S. Wang, J. Chem. Phys. 110 (1999) 8980.
[42] A.M. Manninen, H. Hakkinen, U. Landman, X. Li, L.S. Wang, Phys. Rev. B 60 (1999) 11297.
[43] H. Yoshida, A. Terasaki, K. Kobaysahi, M. Tsukada, T. Kondow, J. Chem. Phys. 102 (1995) 5960.
[44] G. Gantorfor, W. Eberhardt, Phys. Rev. Lett. 76 (1996) 4975.
[45] J. Ho, M.L. Polak, K.M. Ervin, W.C. Lineberger, J. Chem. Phys. 99 (1993) 8542.
[46] K.M. Ervin, J. Ho, W.C. Lineberger, J. Chem. Phys. 89 (1988) 4514.
[47] M.E. Geusic, M.D. Morse, R.E. Smalley, J. Chem. Phys. 82 (1985) 590.
[48] M.D. Morse, M.E. Geusic, J.R. Heath, R.E. Smalley, J. Chem. Phys. 83 (1985) 2293.
[49] S.C. Richtsmeier, E.K. Parks, K. Liu, L.G. Pobo, S.J. Riley, J. Chem. Phys. 82 (1985) 3659.
[50] R.L. Whetten, D.M. Cox, D.J. Trevor, A. Kaldor, Phys. Rev. Lett. 54 (1985) 1494.
[51] E.K. Parks, K. Liu, S.C. Richtsmeier, L.G. Pobo, S.J. Riley, J. Chem. Phys. 82 (1985) 5470.
[52] P.J. Brucat, C.L. Pettiette, L.S. Zheng, M.J. Craycraft, R.E. Smalley, J. Chem. Phys. 85 (1986) 4747.
[53] E.K. Parks, B.H. Weiller, P.S. Bechthold, W.F. Hoffman, G.C. Nieman, L.G. Pobo, S.J. Riley, J. Chem. Phys. 88 (1988) 1622.
[54] D.M. Cox, K.C. Reichmann, D.J. Trevor, A. Kaldor, J. Chem. Phys. 88 (1988) 111.
[55] E.K. Parks, G.C. Nieman, L.G. Pobo, S.J. Riley, J. Chem. Phys. 88 (1988) 6260.
[56] J. Conceicao, R.T. Laaksonen, L.S. Wang, T. Guo, P. Nordlander, R.E. Smalley, Phys. Rev. B 51 (1995) 4668.
[57] I.M.L. Billas, A. Chatelain, W.A. de Heer, Science 265 (1994) 1682.
[58] D.M. Cox, D.J. Trevor, R.L. Whetten, E.A. Rohlfing, A. Kaldor, Phys. Rev. B 32 (1985) 7290.
[59] W.A. de Heer, P. Milani, A. Chatelain, Phys. Rev. Lett. 65 (1990) 488.

[60] J.P. Bucher, D.C. Douglass, L.A. Bloomfield, Phys. Rev. Lett. 66 (1991) 3052.
[61] S. Yang, M.B. Knickelbein, J. Chem. Phys. 93 (1990) 1533.
[62] E.K. Parks, T.D. Klots, S.J. Riley, J. Chem. Phys. 92 (1990) 3813.
[63] E.A. Rohlfing, D.M. Cox, A. Kaldor, K.H. Johnson, J. Chem. Phys. 81 (1984) 3846.
[64] L. Lian, C.X. Su, P.B. Armentrout, J. Chem. Phys. 97 (1992) 4072.
[65] M.B. Knickelbein, J. Chem. Phys. 104 (1996) 3517.
[66] M.B. Knickelbein, G.M. Koretsky, K.A. Jackson, M.R. Peterson, Z. Hajnal, J. Chem. Phys. 109 (1998) 10692.
[67] J. Conceicao, S.K. Loh, L. Lian, P.B. Armentrout, J. Chem. Phys. 104 (1996) 3976.
[68] J.B. Griffin, P.B. Armentrout, J. Chem. Phys. 106 (1997) 4448.
[69] C.Y. Yang, K.H. Johnson, D.R. Salahub, J. Kaspar, R.P. Messmer, Phys. Rev. B 24 (1981) 5673.
[70] K. Lee, J. Callaway, S. Dhar, Phys. Rev. B 30 (1984) 1724.
[71] K. Lee, J. Callaway, K. Kwong, R. Tang, A. Ziegler, Phys. Rev. B 31 (1985) 1796.
[72] G.F. Holland, D.E. Ellis, W.C. Trogler, J. Chem. Phys. 83 (1985) 3507.
[73] G.M. Pastor, J. Dorantes-Davila, K.H. Bennemann, Chem. Phys. Lett. 148 (1988) 459.
[74] G.M. Pastor, J. Dorantes-Davila, K.H. Bennemann, Phys. Rev. B 40 (1989) 7642.
[75] J. Zhao, X. Chen, G. Wang, Phys. Rev. B 50 (1994) 15424.
[76] N.A. Besley, R.L. Johnston, A.J. Stace, J. Uppenbrink, J. Mol. Struct. 341 (1995) 75.
[77] J.L. Chen, C.S. Wang, K.A. Jackson, M.R. Pederson, Phys. Rev. B 44 (1991) 6558.
[78] M. Castro, D.R. Salahub, Phys. Rev. B 47 (1993) 10955.
[79] O.B. Christensen, M.L. Cohen, Phys. Rev. B 47 (1993) 13643.
[80] M. Castra, Int. J. Quant. Chem. 64 (1997) 223.
[81] L.S. Wang, X. Li, in: P. Jena, S.N. Khanna, B.K. Rao (Eds.), Proc. Int. Symp. Clust. Nanostruct. Interf., 25–28 October, 1999, Richmond, VA, World Scientific, NJ, 2000.
[82] L.S. Wang, J. Conceicao, C. Jin, R.E. Smalley, Chem. Phys. Lett. 182 (1991) 5.
[83] H. Weidele, D. Kreisle, E. Recknagel, G.S. Icking-Konert, H. Handschuh, G. Gantefor, W. Eberhardt, Chem. Phys. Lett. 237 (1995) 425.
[84] D.M. Wood, Phys. Rev. Lett. 46 (1981) 749.
[85] A.M. Turner, J.L. Erskine, Phys. Rev. B 25 (1982) 1983.
[86] B. Sinkovic, E. Shekel, S.L. Hulbert, Phys. Rev. B 52 (1995) R8696.
[87] H. Hotop, W.C. Lineberger, J. Phys. Chem. Ref. Data 14 (1985) 731.